PHILOSOPHICAL TRANSACTIONS OF THE ROYAL SOCIETY A MATHEMATICAL, PHYSICAL & ENGINEERING SCIENCES

The Kinetics of Rock Deformation by Pressure Solution [and Discussion]

E. H. Rutter and D. Elliott

Phil. Trans. R. Soc. Lond. A 1976 **283**, 203-219
doi: 10.1098/rsta.1976.0079

Phil. Trans. R. Soc. Lond. A. **283**, 203–219 (1976) [203]
Printed in Great Britain

The kinetics of rock deformation by pressure solution

By E. H. Rutter
Department of Geology, Imperial College, London, S.W.7

A simple model for rock deformation by pressure solution, assuming grain boundary diffusive mass transfer to be deformation rate controlling, is presented. The model leads to a constitutive flow law which is of the same form as that for Coble creep. It is argued that the presence of a fluid film in stressed grain boundaries leads to enhanced diffusivity of solute particles in the grain boundary. Some simple experiments are described, which demonstrate rapid diffusion in solutions in pores, much slower diffusion in stressed interfaces and deformation by pressure solution.

By using the theoretical model, and by assuming that the pressure of the interfacial solution is equal to the applied normal stress, so that available experimental data on the effect of pressure on mineral solubility could be used, rates of deformation by pressure solution have been calculated. These are compared with rates of deformation by crystal plastic and high temperature diffusive flow processes, by using deformation mechanism maps. Predicted transition conditions between various deformation mechanisms are found to be consistent with those inferred from the study of textures of naturally deformed rocks.

Introduction

Several different mechanisms are believed to be important in natural rock deformation, and all are potentially able to produce pseudo steady-state flow. These are:

(*a*) Cataclasis, which involves normal-pressure dependent fracturing, and frictional sliding between rock particles.

(*b*) Dislocation mechanisms, including dislocation glide and dislocation creep. The usage of the latter two terms as names for steady-state flow processes follows their definition by Ashby (1972).

(*c*) Processes which involve shape changes of individual grains by grain boundary or through-the-grain (volume) diffusion, together with a component of grain boundary sliding.

Group *c* includes Coble creep, Nabarro–Herring creep and superplastic flow. There has been some discussion regarding the relative importance of groups *b* and *c* processes in natural rock deformation (Stocker & Ashby 1973; Weertman 1970; Heard & Raleigh 1972; Heard 1972; Raleigh & Kirby 1970; Atkinson 1972, 1975).

The process termed 'pressure solution' (Ramsay 1967; Durney 1972; Elliott 1973; Kerrich 1975; Sorby 1855) appears to be geometrically equivalent to group *c* processes, but in nature it occurs at temperatures lower than those required even for dislocation creep (Kerrich 1975). It seems reasonable to suppose that diffusive mass transport is assisted by the presence of water at grain boundaries – hence the term 'pressure solution'. Effective diffusivities in the aqueous phase may, at temperatures of about 200–400 °C, be of the order of solid state diffusivities at very much higher temperatures.

We will erect a simple model for pressure solution without grain boundary sliding. The model is potentially amenable to experimental study, and some simple experiments designed to investigate some of the characteristics of the theoretical model will be described.

The model

Consider a planar interface subjected to an applied stress σ_a, normal to the interface. The interface contains a high diffusivity (solution) phase and its outer limit is a circle which acts as a sink for solute diffusing out of the interface. The model is of the planar contact between a pair of pill-shaped grains surrounded by saturated solution in contact with the unstressed surfaces. An experimental approximation to this is shown in figure 1, but the interface is connected to the 'sink' solution via a narrow, annular 'pore' space.

Assuming a steady rate of displacement, but no crystal plastic flow or cataclasis, the rate of addition of solid into solution in the interface is constant (A_0) at all points in the interface, and the form of the diffusion equation of interest here is

$$\frac{1}{r}\frac{\mathrm{d}}{\mathrm{d}r}\left(r\frac{\mathrm{d}C}{\mathrm{d}r}\right)+\frac{A_0}{D_b}=0, \tag{1}$$

where C is the concentration at radius r and D_b is the grain boundary diffusivity. It is assumed that solution kinetics are faster than diffusion kinetics, so that diffusion is deformation rate controlling. The solution for the above boundary conditions is (Carslaw & Jaeger 1959, p. 191).

$$C(r) = C_0+(A_0/4D_b)\,(a^2-r^2), \tag{2}$$

where a is the radius of the interface and C_0 is the concentration of the solution outside the interface. Clearly, for steady-state flow, the concentration of the interfacial solution must vary parabolically with radius r. Because the concentration gradient is induced by the normal stress, the latter must vary radially, hence the grain must be heterogeneously stressed, despite the constant orientation of the interface. Because of the requirement that forces normal to the interface must be in equilibrium, we can write

$$\sigma_a a^2 = 2\int_0^a \sigma(r)\, r\, \mathrm{d}r. \tag{3}$$

Next, interfacial solution concentration must be related to normal stress. Paterson (1973) has shown that, to a first approximation, the chemical potential, μ, of a solute in an unstressed solution phase in equilibrium with stressed solid is given by $\mathrm{d}\mu = V\,\mathrm{d}\sigma/RT$, where σ is the stress normal to the interface, R is the gas constant, T is the absolute temperature and V is the molar volume of the crystalline solid. Making use of the explicit form of the chemical potential, $\mathrm{d}\mu = RT\,\mathrm{d}\ln\gamma C$, where γ is a ratio of activity coefficients, we can write

$$V\sigma(r) = RT\,(\ln(C(r)/C_0)+\ln\gamma), \tag{4}$$

where C_0 is the concentration of a saturated solution in equilibrium with unstressed solid. For simplicity, we assume ideal solution behaviour ($\gamma = 1$), though the procedure is not much more complicated if non-ideal behaviour is considered. Thus equation (3) becomes

$$\sigma_a = \frac{2RT}{a^2V}\int_0^a r\ln\left[1+\frac{A_0}{4C_0D_b}\,(a^2-r^2)\right]\mathrm{d}r. \tag{5}$$

At low stresses ($\sigma_a < 30$ MPa), the approximation $y = \ln(1+x) \simeq x$ may be used and the integral evaluated simply. Substituting $A_0 = 2a\dot{e}\rho/w$, where $\dot{e}$ is the strain rate, assuming that pressure solution occurs at every grain boundary in a polycrystalline aggregate, so that

PHILOSOPHICAL TRANSACTIONS OF THE ROYAL SOCIETY A MATHEMATICAL, PHYSICAL & ENGINEERING SCIENCES

displacement rate at a single interface can be related to strain rate for the aggregate, ρ is the density of the solid and w is the effective width of the grain boundary, we obtain

$$\dot{e} = \frac{32\sigma_a VC_0 D_b w}{RT\rho d^3}, \tag{6}$$

where $d = 2a$, the grain diameter. Equation (6) is of the same form as the equation for Coble creep (Coble 1963; Raj & Ashby 1971).

At high stresses ($\sigma_a > 100$ MPa) the approximation $y = \ln(1+x) \approx \ln x$ may be used and the integrand becomes

$$\sigma_a = 2.303 \frac{RT}{V} \lg\left[\frac{d^3\dot{e}\rho}{40C_0 D_b w}\right]. \tag{7}$$

Equations (6) and (7) are approximately simultaneously satisfied by

$$\sigma_a = \frac{RT}{V} \operatorname{arsinh}\left[\frac{d^3\dot{e}\rho}{40C_0 D_b w}\right]. \tag{8}$$

There are no suitable experimental data by which this model might be tested. In particular, there are no data on the effect of pressure on a solid on the solubility of that solid in a solvent which is not subjected to the same pressure. In contrast, there are experimental data on the effect of total pressure on the solubility of minerals like quartz (Kennedy 1950; Holland 1967) and calcite (Sharp & Kennedy 1965), when the solvent is subjected to the same pressure as the crystalline solid. In this case it is well known that total pressure affects solubility according to the relation (Zen 1957)

$$\left(\frac{\partial C}{\partial p}\right)_T = \frac{V - V_L}{(\partial\mu/\partial C)_{T,p}}, \tag{9}$$

where $(\partial C/\partial p)_T$ is the pressure coefficient of solubility and V_L is the partial molar volume of the solute in the solution phase. Note that this partial molar volume does not appear in the expression for the stress coefficient of solubility of a solid in contact with unstressed solution, thus it does not appear in equations (6), (7) and (8). Despite the inaccuracies which may be introduced, it may still be of interest to compute rates of deformation by pressure solution using the available experimental data. This may be less unsatisfactory than making the assumption that the ratio of activity coefficients, γ, equals unity, as in the purely theoretical treatment given above.

The interfacial fluid

The use of experimental data such as that mentioned above presumes that an aqueous solution can exist within a stressed interface. There is a great deal of evidence that thin, adsorbed films of liquid can exist between stressed surfaces, and that such films possess anomalous physical properties. The mechanical properties of very thin surface films sandwiched between bearing surfaces are of great interest in lubrication practise (Roberts & Tabor 1970). Geological evidence suggests that the presence of clay along stylolites may increase the rate of pressure solution (Heald 1956), in contrast to the inhibiting effect of second phase particles in grain boundaries on the rate of high temperature solid state diffusion creep (Harris 1973). The presence of clay along stylolites will increase the effective grain boundary width (Weyl 1959). Also, it is well known that clays, better than most minerals, adsorb polar molecules and cations to balance charges due to substitution within the structure and due to broken bonds (Ward

& Fraser 1967). Electrical conduction by ionic diffusion in clays and clay rich rocks is thereby enhanced. Further, once a concentration gradient has been set up in an interfacial 'solution', the fluid pressure in the interface will tend to rise to restore osmotic equilibrium. Equilibrium osmotic pressure is given (Hanshaw & Zen 1965) by

$$\delta p = \frac{RT}{V_{H_2O}} \ln \left[\frac{\alpha'_{H_2O}}{\alpha''_{H_2O}}\right], \tag{10}$$

where δp is the osmotic pressure difference across a membrane between two solutions of different concentrations, V_{H_2O} is the molar volume of water and α'_{H_2O} and α''_{H_2O} represent the activities of water in the weak and stronger solutions respectively. If applied stress produces a change in concentration $C(r)$, osmotic pressures commensurate with $\sigma(r)$ might be expected to arise. Hanshaw & Zen (1965) point out that osmotic pressure differences of the order of 50 MPa might be expected across clay rich layers in rock sequences, and that the development of such pressures may be important in the location and initiation of faulting. Elevated fluid pressures produced during deformation by pressure solution would be expected to facilitate such grain boundary sliding as might be required during the deformation of a polycrystalline aggregate in order to maintain strain compatibility. The above points help to justify the use of experimental data on the effect of total solvent pressure on solubility in pressure solution calculations.

The rate of strain produced by pressure solution is highly sensitive to the diffusivity, D_b, of dissolved particles in the interfacial solution film. To a reasonable approximation, the diffusivity, D, of a solute particle in a large volume of solution is given by the Stokes–Einstein equation

$$D = RT/6\eta \sqrt[3]{V}, \tag{11}$$

where $\eta = \eta_0 RT \exp(H/RT)$ in which η is the viscosity of the pure solvent, η_0, is a constant and H is an activation enthalpy. Despite the fact that in its derivation this equation strictly relates to the motion of large spheres through a continuous fluid, it predicts the diffusivities of a wide range of solute particles in liquids to within one order of magnitude (Jost 1960). Frenkel (1946) discusses the physical basis of the relation using the kinetic theory of liquids, and shows that a single diffusive jump of a solute particle into a neighbouring liquid 'hole' involves the concomitant motion of many surrounding solvent particles. However, it is well known from experiment that the apparent viscosity of a polar liquid in a thin film between solid surfaces is much greater than in large liquid volumes (Churayev *et al.* 1970; Henniker 1949). This is due to the phenomenon of electroviscosity (McGregor 1974, p. 153). Polar molecules adsorbed on liquid surfaces have an ordered structure relative to the bulk fluid, so that shearing displacements generate an electric potential gradient which opposes the force producing the displacement. A corresponding reduction in the diffusivity of particles in the interfacial liquid may therefore be expected. By a neutron scattering technique, Olejnick *et al.* (1970) have shown that self diffusivity of interlayer water in various sheet silicates is markedly reduced compared with bulk liquid diffusivity.

Apparent viscosity, η_a, in thin films when the electroviscous effect is significant (film thickness less than 10^{-6} m) is given by (Elton 1948)

$$\eta_a = \eta + 3\epsilon^2\psi^2/8\pi^2 k w^2, \tag{12}$$

where ϵ is the dielectric constant, ψ the electrokinetic potential and k the specific electrical conductivity, of the liquid, and w is the thickness of the liquid film. Using the values given by

PHILOSOPHICAL TRANSACTIONS OF THE ROYAL SOCIETY A MATHEMATICAL, PHYSICAL & ENGINEERING SCIENCES

Elton for water, the apparent viscosity for a 2 nm layer is 10^{+5} of the value for the bulk fluid. In calculating rates of deformation by pressure solution, it was therefore assumed that D_b is less than D by a factor of 10^{-5}. Thus at room temperature, D_b is of the order of 10^{-10} cm^2 s^{-1} for pressure solution. By contrast, solid state grain boundary diffusivities for minerals at the same temperature are expected to be about ten orders of magnitude smaller again.

Several complicating factors can conspire to make the calculated diffusivity multiplier of 10^{-5} for pressure solution either too large or too small. A discussion of such factors is beyond the scope of the present article. I believe that uncertainty in the value of this multiplier represents the main source of uncertainty in calculated strain rates due to pressure solution.

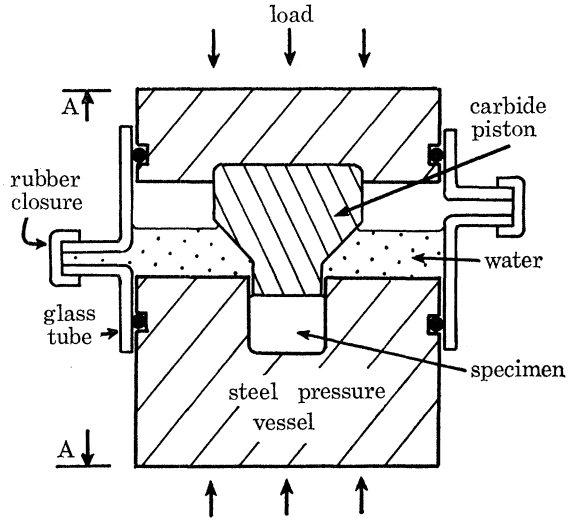

FIGURE 1. Schematic cross section through apparatus used to study deformation rates by pressure solution (not to scale). Displacements are measured using an electromechanical transducer between points A–A. The tungsten carbide piston, resting on a compacted powder specimen, is 0.5 cm in diameter. The portion of the apparatus shown here is about 6 cm high, and fits between the loading platens of a creep testing machine.

EXPERIMENTS

Several simple tests at room temperature have been performed in order to investigate some of the problems of devising an experimental approach to the study of pressure solution, and to explore some of the points in the theoretical model. Ideally, experiments should be devised in which materials are deformed only by pressure solution, other mechanisms of deformation, such as crystal plasticity and cataclasis, being suppressed. To approach this end, a hydrostatic compaction apparatus, figured schematically in figure 1, was constructed. A solid, in the form of a crystalline powder, could be compacted in the pressure vessel until detectable deformation ceased. Stresses up to 1200 MPa could be applied. High stresses were used to ensure that pore spaces were eliminated. Thus deformation at constant volume was inhibited. The only way in which the loading piston could advance into the pressure vessel was by removal of sample material from within the pressure vessel. In all of these experiments a thin layer of montmorillonite was placed between the specimen and the loading piston.

By adding water into the annular space around the loading piston, pressure solution, due to dissolution and diffusion of material along the interface, might be expected to occur; dissolved material being accumulated in dilute solution in the water around the loading piston. In

practice, it was found that within minutes of adding water, steady state flow at a constant rate of piston displacement developed. Figure 2 shows displacement/time data for three salts. Qualitatively, displacement rate is greater, the higher the solubility of the salt. In order to check that this effect is not simply water-induced further compaction, some experiments were performed using ^{14}C labelled solid sodium carbonate as the specimen. The middle group of data in figure 3 show that the amount of ^{14}C dissolved in the 2.0 ml of water around the piston was proportional

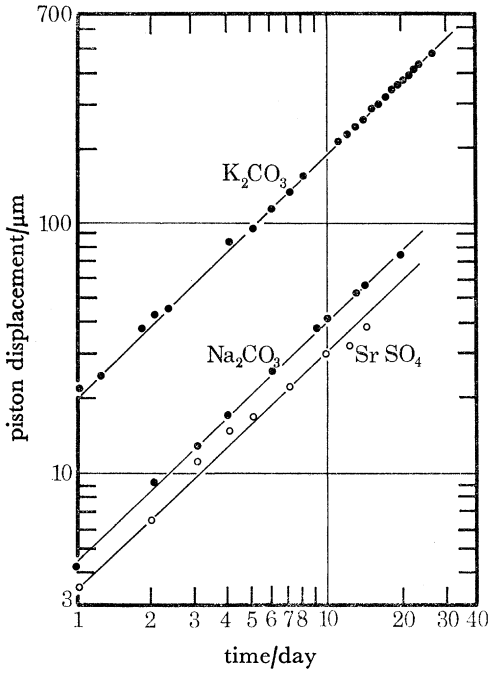

FIGURE 2. Steady-state 'flow' in three salts tested in the compaction apparatus at 880 MPa normal stress. Before water had been introduced into the apparatus the salts had been compacted until piston displacement ceased. Relative solubilities of these salts are $K_2CO_3 > Na_2CO_3 > SrSO_4$.

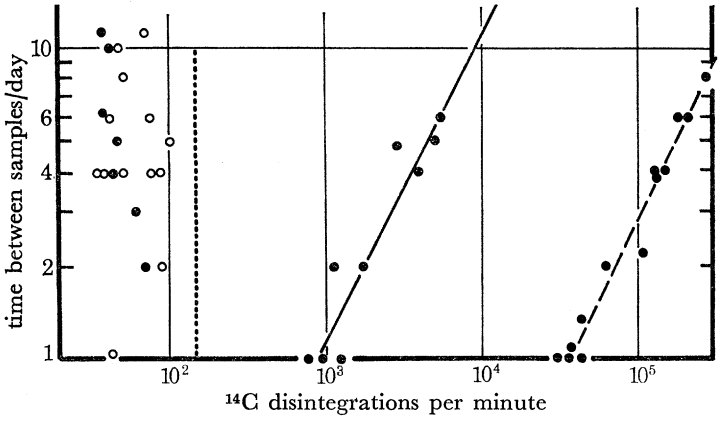

FIGURE 3. Some results of the radioisotopic tracer experiments. The left hand data points show insignificant diffusion along a stressed interface (the dashed vertical line represents the limit of significant resolution; ●, 880 MPa; ○, 100 MPa). The right hand data points relate to diffusion of ^{14}C labelled Na_2CO_3 in solution through a 25 μm wide 'pore'. The time between sampling is proportional to the amount of salt diffused. The central data points show the correlation between mass diffused in a deformation experiment (proportional to sample radioactivity) and mass diffused calculated from mechanical measurements of piston displacement (continuous line); 880 MPa.

to the time elapsed between observations. The continuous line drawn through these points is the rate of transfer of ^{14}C inferred from the mechanical displacement data. There is good correlation between the two kinds of data. Technical details relating to the isotopic tracer method are given in the appendix.

The far right group of data in figure 3 show radioisotopic measurements of diffusion of $Na_2{}^{14}CO_3$ through the annular region between piston and pressure vessel wall. The same setup was used for these experiments as for the deformation experiments except that the solid was unstressed. Diffusivities calculated from these data were of the order of 10^{-5} cm^2 s^{-1}, which is typical for the diffusion of salts in large volumes of water (this result can also be obtained from the Stokes–Einstein equation). Thus diffusion through a 'pore' 25 μm wide does not lead to any electroviscous effect.

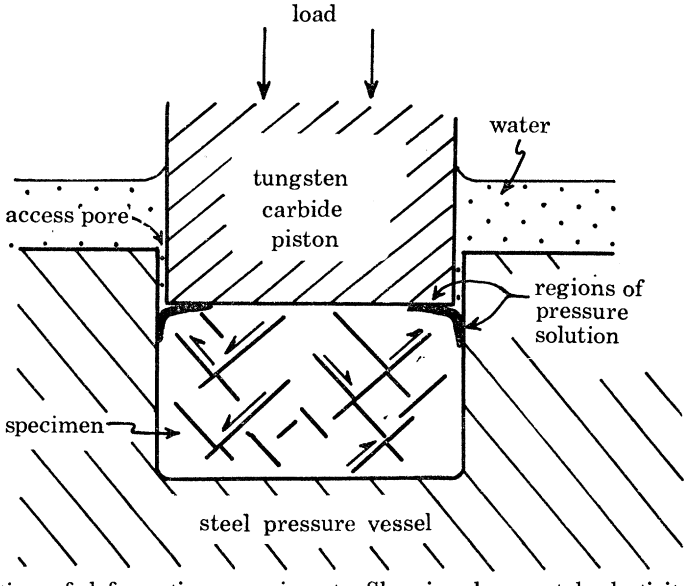

FIGURE 4. Interpretation of deformation experiments. Shearing by crystal plasticity and brittle fracture supplies mass to the peripheral region of the sample where pressure solution occurs. The sample geometry remains constant during deformation, hence a constant piston displacement rate results.

At the other extreme, the far left group of data in figure 3 show the results of attempts to measure the product $D_b w$ along interfaces subject to stresses ranging from 50 to 1000 MPa and a solution concentration gradient. In all cases the amount of ^{14}C transferred was below the limit of significant resolution, and there is no systematic time dependence of mass transferred. From this it was inferred that for a stressed interface $D_b w$ is less than 10^{-11} cm^3 s^{-1}. Radioisotopic concentrations thousands of times greater than those used in the present experiments would be required to measure stressed grain boundary diffusivity directly.

It has been shown that for steady flow by pressure solution, the normal stress across a planar interface is heterogeneous. Thus it is likely that in these deformation experiments transfer of mass into the 'pore' space region occurs partly by pressure solution in the outer portion of the interface and partly through shearing by cataclasis and crystal plasticity, as suggested in figure 4. It is possible that such a combined process is important in some natural rock deformation. The nominal piston diameter in these experiments was 0.5 cm, and it can be argued from the theory given earlier that pressure solution alone over such a large 'grain' size would not produce the observed displacement rates. However, because steady-state flow was observed, and because

PHILOSOPHICAL TRANSACTIONS OF THE ROYAL SOCIETY A MATHEMATICAL, PHYSICAL & ENGINEERING SCIENCES

'pore' diffusion was shown to be relatively fast compared with the $Na_2{}^{14}CO_3$ transport rates observed in the deformation experiments, it is probable that the overall rate of deformation is controlled by diffusion in the outer portion of the stressed interface. A further point in support of this suggestion is that a stress dependence of displacement rate (figure 5) was observed. This figure shows combined data from four separate experiments on Na_2CO_3. The exponential form of the stress dependence at high stresses is as predicted by equation (7). Provided that the pressure solution involves an interfacial solution phase with pressure equal to the applied stress, the slope of the graph is given by $(V-V_L)/RT$. From Zen's (1957) tables of partial molar volumes of common salts it can be shown that the observed slope of the graph is consistent with an average solution concentration of 400 g/l, which is about twice the concentration of a saturated solution of sodium carbonate (Stephen 1963) under atmospheric pressure.

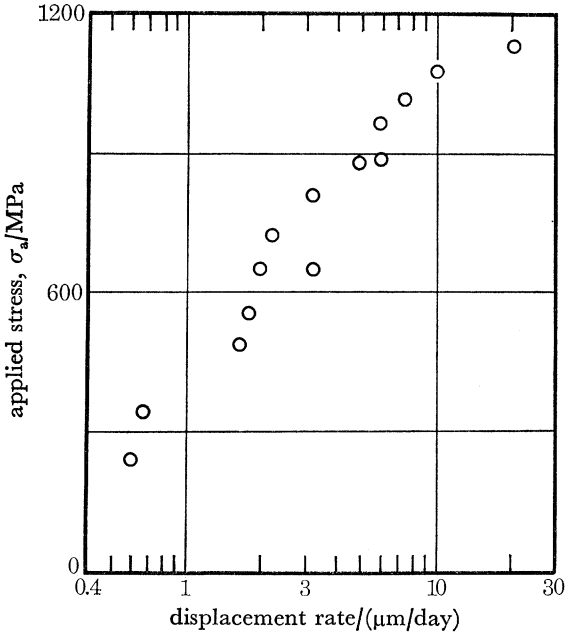

FIGURE 5. The stress dependence of piston displacement rate in deformation experiments.

COMPARISON OF PRESSURE SOLUTION WITH SOLID STATE DIFFUSION CONTROLLED CRYSTAL PLASTICITY

By using equations (6), (7) and (8) rates of pressure solution for polycrystalline minerals can be calculated. Such data can be conveniently plotted as contours of strain rate in a stress against temperature coordinate frame. In the same diagram, data for flow by dislocation glide, dislocation creep, Nabarro–Herring creep and Coble creep may be plotted (deformation mechanism map of Ashby (1972), similar concept outlined by Weertman (1968)). Fields in stress/temperature space where strain rate is dominated by a particular mechanism are bounded by lines along which the strain rates contributed by the two different mechanisms in adjacent fields are the same. Such diagrams have two important uses:

(*a*) For any specified pair of the variables, strain rate, temperature or stress, the value of the third one may be read directly from the deformation mechanism map.

(*b*) The conditions of strain rate, temperature and stress which must be applied to a rock in order to study a particular deformation mechanism can be quickly read from the map. One of the purposes of the present study was to develop a feeling for an experimental approach to pressure solution as a deformation mechanism.

Deformation mechanism maps for quartz and calcite have been constructed. For the crystal plastic flow fields the following equations were used. For both quartz and calcite the equation (Bird, Mukherjee & Dorn 1969)

$$\dot{e}_{11} = A \frac{D_v G b}{RT} \left(\frac{\sigma_{11}}{G}\right)^n \tag{13}$$

was used to represent the dislocation creep behaviour and

$$\dot{e} = 21 \frac{V \sigma D_v}{RT\, d^2} \left(1 + \pi \frac{w}{d} \frac{D_b}{D_v}\right) \tag{14}$$

was used to represent Nabarro–Herring and Coble creep (Raj & Ashby 1971). In these equations D_v and D_b are volume and grain boundary diffusivities respectively, and are related to temperature by $D_j = D_0 \exp(-H_j/RT)$; $j = v$ or b, where D_0 is a constant and H_j is the heat of activation. A and n are dimensionless parameters, V is the activation volume, here assumed equal to the molar volume, and G is the shear modulus.

For flow by dislocation glide, a flow law of the form $\dot{e} = B \exp(-(H - \sigma V)/RT)$ was used for calcite (Rutter 1974). For quartz, in the absence of suitable data, straight strain rate contours have been drawn assuming that at absolute zero of temperature the strength of quartz equals $\frac{1}{10}G$, and that the transition to dislocation creep occurs at $10^{-3}\,G$ (Weertman 1968). The straight line approximation is regarded as acceptable because most of the dislocation glide field may be expected to lie outside the region of geological interest.

Values of the various parameters used in all the equations are listed in the appendix. Strain rates due to combinations of mechanisms were regarded as additive, except for dislocation glide and dislocation creep, which are mutually exclusive. In constructing the deformation maps, 'experimental' differential stress and strain rates were used for simplicity, rather than the second invariants of the deviatoric stress and strain rate tensors. The latter parameters relate to more general flow geometries and it is a simple matter to modify the deformation map accordingly. Nye (1953) has discussed the problem of relating stress and strain rate in different flow geometries.

Figures 6 and 7 show computed deformation maps for crystal plastic flow in calcite and quartz, and figures 8 and 9 show the effects of introducing a pressure solution field. Following Nye (1953) differential stress has been related to shear modulus by a factor $1/\sqrt{3}$ in the left hand ordinate. The pressure solution and diffusive mass transfer flow fields were both computed assuming 100 μm grain size. The effect of reducing the grain size to 10 μm is to increase strain rates by 100 times in the Nabarro–Herring creep field and by 1000 times in the Coble creep and pressure solution flow fields (see also contributions by Watterson and by White, this volume). This increases the size of these fields at the expense of the dislocation flow fields. Possible grain size effects in the dislocation flow fields have been neglected.

The curious sinusoidal shape of the strain rate contours in the pressure solution field for calcite arises because of the competing effects of decreasing C_0 and increasing rate of change of solubility with pressure as temperature is increased. In the case of quartz, the pressure solution/solid state diffusion creep boundary at low stresses has been drawn at 650 °C on the assumption

PHILOSOPHICAL TRANSACTIONS OF THE ROYAL SOCIETY A MATHEMATICAL, PHYSICAL & ENGINEERING SCIENCES

that in natural rocks most of the available water will become either dissolved in small quantities of quartzo-feldspathic liquid, or reduced to a very low concentration through the increase in molar volume of water with temperature at constant pressure, thus inhibiting pressure solution.

A significant test of the validity of the concepts outlined in this paper is that predicted strain rates within the regime of geological interest (stresses between 1 and 100 MPa and temperatures between 100 and 800 °C) should accord with likely values of this parameter during orogenesis (10^{-14}–10^{-11} s^{-1}, Price 1970, 1975; Heard & Raleigh 1972). Further, predicted

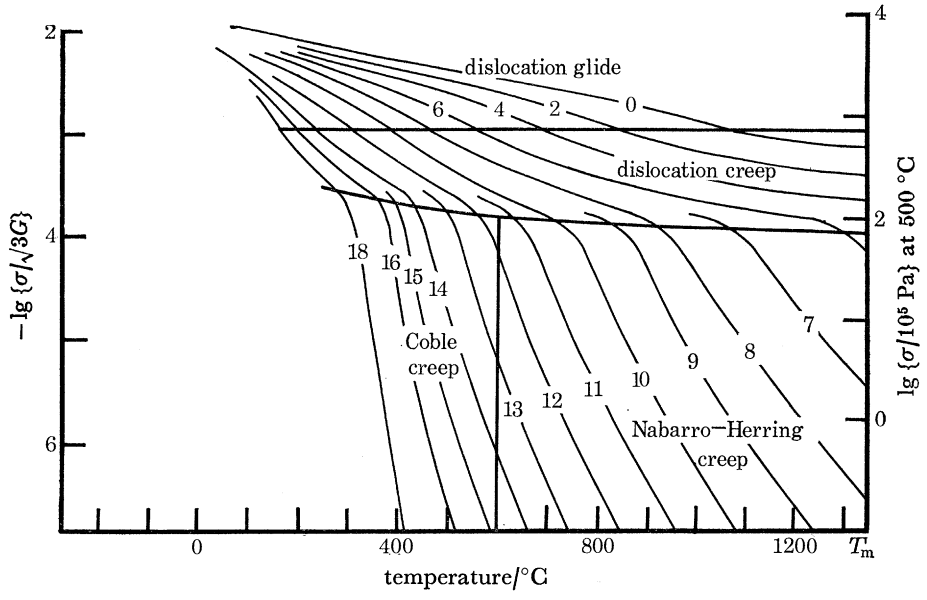

FIGURE 6. Deformation mechanism map for calcite without pressure solution. Contours of −lg strain rate are shown. σ is differential stress $(\sigma_{11}-\sigma_{33})$. $d = 100$ μm; $V = 37$ cm³.

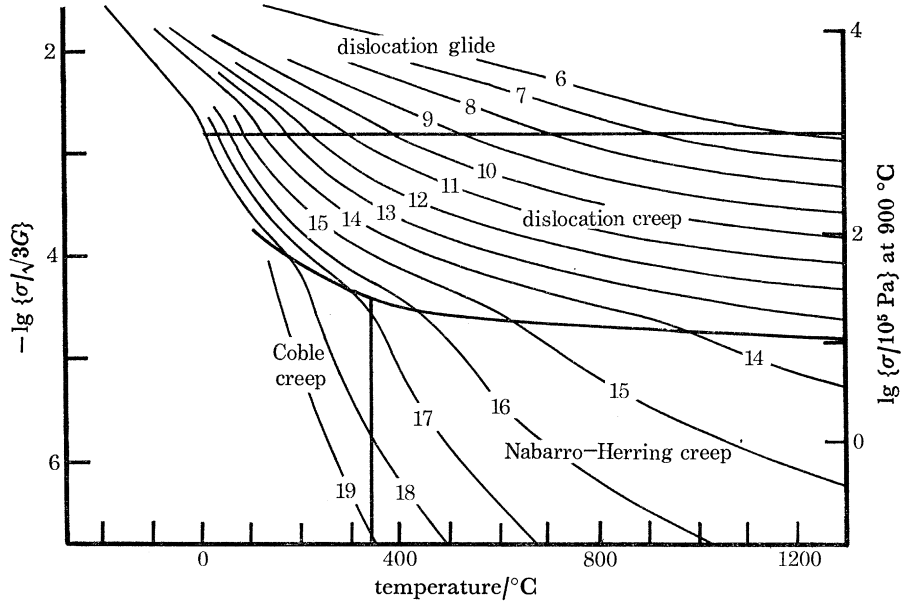

FIGURE 7. Deformation mechanism map for quartz without pressure solution. Contours of −lg strain rate are shown. σ is differential stress $(\sigma_{11}-\sigma_{33})$. $d = 100$ μm; $V = 22$ cm³.

predominant mechanisms of deformation should correspond with those inferred from studies of natural tectonites by optical and electron microscopy. On both accounts the predictions contained in these diagrams seem valid. Most geologists would agree that textures characteristic of diffusive mass transfer by pressure solution are common in rocks deformed at temperatures up to about 400 °C, and that crystal plastic flow textures dominate at high temperatures (White, this volume; Kerrich 1975; Ramsay 1967; Durney 1972; Rutter 1974).

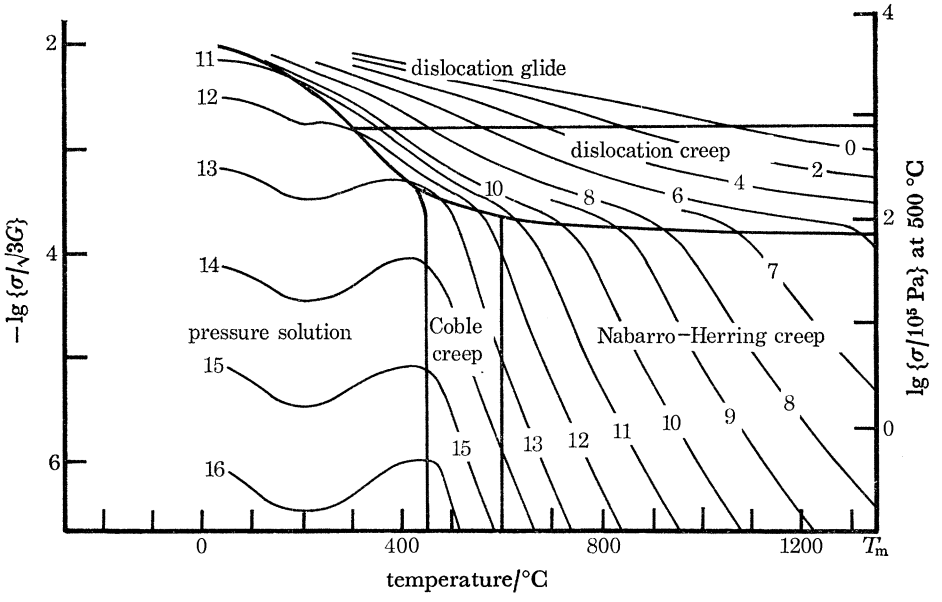

FIGURE 8. Deformation mechanism map for calcite modified by the addition of a pressure solution field. $d = 100\ \mu m$; $V = 37\ cm^3$.

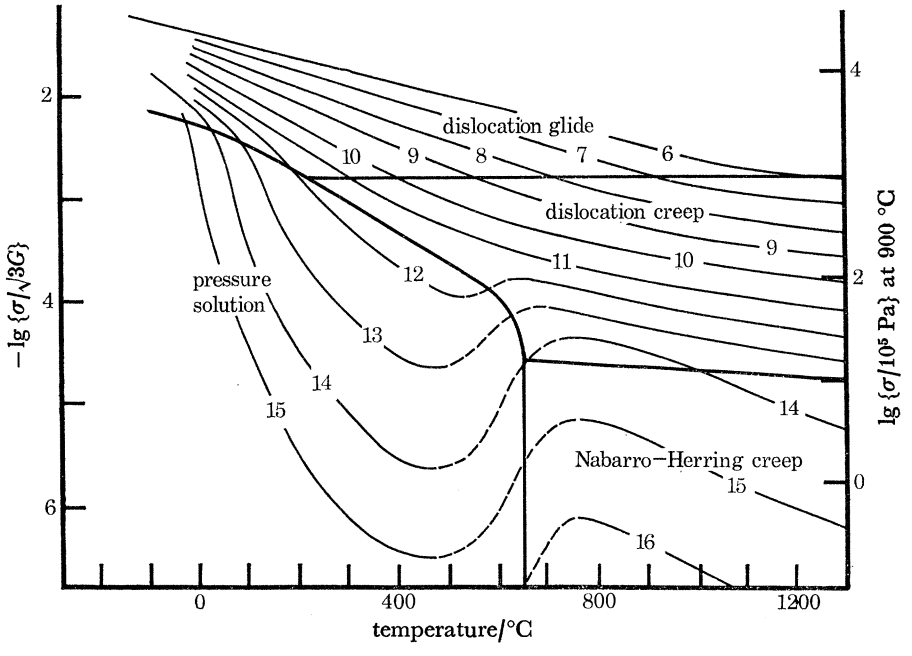

FIGURE 9. Deformation mechanism map for quartz modified by the addition of a pressure solution field. The region of dashed strain rate contours represents the inhibition of pressure solution through decrease in pore water concentration. $d = 100\ \mu m$; $V = 22\ cm^3$.

Appendix

Data for the construction of deformation mechanism maps

(a) Calcite

(i) *Crystal plastic flow*

An activation enthalpy of 250 kJ mol^{-1} was assumed representative of the diffusion of species controlling deformation rate (Heard & Raleigh 1972; Rutter 1974) at $T > 400$ °C and 197 kJ mol^{-1} at $T < 400$ °C (Rutter 1974). The volume diffusivity at 1100 °C was assumed to be equal to the figure obtained by Anderson (1969) at the same temperature, namely, 1×10^{-11} s^{-1} cm^2, thus $D_0 = 5 \times 10^{-2}$ cm^2 s^{-1}. These figures result in a value for A in equation (13) which is consistent wih the empirical relation between A and n postulated by Stocker & Ashby (1973), when applied to the experimental data of Heard & Raleigh (1972). Following Stocker & Ashby (1973), D_0 for grain boundary diffusion was assumed equal to D_0 for volume diffusion and the activation enthalpy two thirds of that for volume diffusion. The relatively large ratio $H_b/H_V = \frac{2}{3}$ tends to compensate for the fact that D_0 for grain boundary diffusion is usually less than D_0 for volume diffusion. The grain boundary width for Coble creep was taken to be 1 nm. With these assumptions, the Coble creep – Nabarro–Herring creep boundary lies at 600 °C. It may be noted that reducing H_b/H_V or decreasing the grain size raises the transition temperature considerably. Activation volume for diffusion was assumed equal to the molar volume at atmospheric pressure. Variations of molar volume with temperature and pressure were neglected.

Birch (1966) gives shear modulus data and the temperature dependence is given by Dandekar (1968).

(ii) *Pressure solution*

In the pressure solution calculations, it was assumed that because of the osmotic pressure effect, interfacial fluid pressure would approach the local solid–solid normal stress, so that published data on the effect of total solvent pressure on solubility could be used. Analysis of data presented by Sharp & Kennedy (1965) on the solubility of calcite in water gave the following relation between solubility, S (mass %), pressure, p (Pa), and temperature, T (°C), of the solution

$$\lg S = A + BT + CpT + Dp, \tag{A 1}$$

where $A = 2.06$, $B = 0.0145$, $C = 0.00006$, $D = -0.0075$.

This relation is valid between 130 and 400 °C when 4.0 mass % of CO_2 is dissolved in the solution. Sharp & Kennedy showed that the solubility of calcite in CO_2 solution is a maximum and is fairly constant in the range 2–6 mass % CO_2. For these calculations the reference pore fluid pressure was taken to be 100 MPa so C_0 is the solubility of calcite in CO_2 solution at this pressure. C_0 also depends upon T. Therefore

$$\lg (C(r)/C_0) = (CT + D)\,(\sigma(r) - p), \tag{A 2}$$

and the flow law can be derived from

$$2.303\,(\sigma_a - p)\,(CT + D) = \frac{2}{a^2}\int_0^a r \ln\left[1 + \frac{\dot{e}\rho d}{4D_b w C_0}\,(a^2 - r^2)\right] \mathrm{d}r. \tag{A 3}$$

The flow law at low stresses becomes

$$\dot{e} = 74(\sigma_a - p)\,D_b w C_0 (CT + D)/\rho d^3. \tag{A 4}$$

Following Weyl (1959) the effective grain boundary width was taken to be 2 nm. Taking into

account the electroviscous effect, D_b in the interface at 0 °C was taken to be 10^{-10} cm^2 s^{-1}. The activation enthalpy for diffusion in water was calculated from viscosity data for water (Lawson & Hughes 1963) and found to be 13.4 kJ mol^{-1}. It is assumed that this figure is the same for thin liquid films as for large liquid volumes. The low value for H means that diffusivity does not depend greatly on temperature. The effect of substantial hydrostatic pressure change is even less marked, and has been neglected in this study.

(*b*) *Quartz*

It was assumed that the activation enthalpy associated with intracrystalline deformation was of the order of that for OH^- and H^+ diffusion (84 kJ mol^{-1}) and that quartz deforms in nature in a 'hydrolytically weakened' state (Griggs 1967). It was clear, however, that observed diffusivities of OH^- and H^+ in quartz (White 1971; Kats 1962) are far too high to control deformation rates. To locate initially the strain rate contours, an experimental result by Tullis *et al.* (1973), in which recovery textures were produced in a natural quartzite, was used. This result gives a strain rate of 10^{-7} s^{-1} at 100 MPa differential stress at 900 °C. This stress level was assumed to lie at the boundary between dislocation glide and dislocation creep fields (the stress level being of the expected order of magnitude). For dislocation creep a value $n = 4$ was adopted, based partly on Balderman's (1974) figure of 3.64 for hydrolytically weakened quartz at 500 °C, and on a value of 4.2 calculated from stress relaxation data for synthetic quartz deformed at 900 °C (Hobbs 1968) by using the relation

$$n = 1 - (\partial \lg t / \partial \lg \sigma), \tag{A 5}$$

where t is the time associated with stress σ.

By using $n = 4$, the dimensionless constant A in equation (13) was calculated from the empirical relation $n = 3.07 + 0.29 \lg A$, given by Stocker & Ashby (1973). The volume diffusivity corresponding to Tullis's 900 °C experiment was then calculated using the dislocation creep equation (13), and found to be 1.2×10^{-17} cm^2 s^{-1}. Assuming H for deformation to be 84 kJ mol^{-1}, D_0 becomes 4×10^{-14} cm^2 s^{-1}. The assumed relation between grain boundary and volume diffusivities was as for calcite.

Burgers vector, b, for quartz was taken to be 0.5 nm (White 1974, personal communication) and effective grain boundary width for Coble creep as $2b$. The shear modulus at 20 °C for quartzite was taken to be 42 GPa (Birch 1966) and its temperature coefficient as given by Baeta & Ashbee (1970) 2.17×10^{-4} K^{-1} at 800 °C.

In the pressure solution calculations the effect of temperature and hydrostatic pressure of the solution on solubility was obtained from Smith (1963) and Holland (1967), who summarize data obtained by several workers. Nearly all of the observed temperature and pressure effects are due to the combined effects of these variables on the molar volume of water. Between 100 and 500 °C

$$\lg S \text{ (mass \%)} = E - 10^3/T + F\Delta p, \tag{A 6}$$

where Δp is the excess pressure (Pa) above a reference pressure of $p = 100$ MPa at temperature T(K). $F = 0.0018$ and $E = 0.46$. From equation (A 6), $\lg (C(r)/C_0) = F(\sigma - p)$, and the flow law at low stressses becomes

$$2.303\, F(\sigma_a - p) = \dot{\epsilon} \rho d^3 / 32\, D_b\, w\, C_0. \tag{A 7}$$

In all other respects the assumptions made in the pressure solution calculations for calcite were applied to quartz.

Isotopic tracer experiments

^{14}C labelled sodium carbonate was prepared by evaporating to dryness a solution containing 40 g unlabelled Na_2CO_3 to which 1 mCi of labelled solution had been added. The resulting powder was used directly in the compaction experiments.

Periodically during each run, a hypodermic syringe was used to withdraw 1.0 ml samples of labelled solution from experiments. The activity of each solution was determined using a Packard Tri-Carb liquid scintillation spectrometer. The scintillant used for each sample was 10 ml of stock solution, prepared by dissolving 50 g naphthalene plus 3.0 g butyl-PBD in 500 ml toluene. To each sample 9.0 ml of ethylene glycol monomethyl ether was added as an incorporation aid. Results were corrected for the quenching effect of water and the incorporation agent, but a time dependent decay of apparent activity was observed over several weeks after the aqueous solution had been added to the scintillant. This is believed due to a slow reaction between the Na_2CO_3 and the components of the scintillant cocktail, leading to progressive reduction of scintillation efficiency. This effect, coupled with experimental problems of accurate volumetric sampling, has meant that the isotopic tracer experiments are only of semi-quantitative significance.

Thanks are due to Dr S. White and Dr B. K. Atkinson for discussion and critical reading of the manuscript. R. F. Holloway and I. T. Morton assisted with apparatus construction. Scintillation counting facilities were provided by Imperial College Biochemistry Department. This work forms part of an experimental investigation of rock deformation processes financed by the Natural Environment Research Council.

References (Rutter)

Ashby, M. F. 1972 A first report on deformation mechanism maps. *Acta Metall.* **20**, 887–897.

Anderson, T. F. 1969 Self-diffusion of carbon and oxygen in calcite by isotope exchange with carbon dioxide. *J. geophys. Res.* **74**, 3918–3932.

Atkinson, B. K. 1972 Ph.D. Thesis, University of London.

Atkinson, B. K. 1975 The temperature and strain rate dependent mechanical behaviour of a polycrystalline galena ore. Submitted to *Economic Geol.*

Baeta, R. D. & Ashbee, K. H. G. 1970 Mechanical deformation of quartz. 2. Stress relaxation and thermal activation parameters. *Phil. Mag.* **22**, 624–635.

Balderman, M. A. 1974 The effect of strain rate and temperature on the yield point of hydrolytically weakened synthetic quartz. *J. geophys. Res.* **79**, 1647–1652.

Birch, F. 1966 Elastic constants and compressibility. In *Handbook of physical constants* (ed. S. P. Clark, Jr.). *Mem. geol. Soc. Am.* **97**.

Bird, J. E., Mukherjee, A. K. & Dorn, J. E. 1969 Correlations between high temperature creep behaviour and structure. In *Quantitative relation between properties and microstructure*. Israel University Press.

Carslaw, H. S. & Jaeger, J. C. 1959 *Conduction of heat in solids*. Oxford: Clarendon Press.

Churayev, N. V., Sobolev, V. D. & Zorin, Z. M. 1970 Measurement of viscosity of liquids in quartz capillaries. In Thin liquid films and boundary layers, *Spec. Discuss. Faraday Soc.* **1**, 213–220.

Coble, R. L. 1963 A model for boundary diffusion controlled creep in polycrystalline materials. *J. appl. Phys.* **34**, 1679–1682.

Dandekar, D. P. 1968 Variation in the elastic constants of calcite with temperature. *J. appl. Phys.* **39**, 3694–3699.

Durney, D. W. 1972 Solution-transfer, an important geological deformation mechanism. *Nature, Lond.* **235**, 315–317.

Elliott, D. 1973 Diffusion flow laws in metamorphic rocks. *Geol. Soc. Am. Bull.*, **84**, 2645–2664.

Elton, G. A. H. 1948 Electroviscosity: the flow of liquids between surfaces in close proximity. *Proc. R. Soc. Lond.* A **194**, 259–274.

Frenkel, J. 1946 Kinetic theory of liquids. New York: Dover.

PHILOSOPHICAL TRANSACTIONS OF THE ROYAL SOCIETY A MATHEMATICAL, PHYSICAL & ENGINEERING SCIENCES

Griggs, D. T. 1967 Hydrolytic weakening of quartz and other silicates. *Geophys. J. R. Astron. Soc.* **14**, 19–31.
Hanshaw, B. B. & Zen, E-an. 1965 Osmotic equilibrium and overthrust faulting. *Geol. Soc. Am. Bull.* **76**, 1379–1386.
Harris, J. E. 1973 The inhibition of diffusion creep by precipitates. *Metals Sci. J.* **7**, 1–6.
Heald, M. T. 1956 Cementation of Simpson and St. Peter sandstones in parts of Oklahoma, Arkansas and Missouri. *J. Geol.* **64**, 16–30.
Heard, H. C. 1972 Steady-state flow in polycrystalline halite at pressure of 2 Kilobars. In Flow and fracture of rocks (The Griggs Volume) (ed. H. C. Heard & others). *Am. Geophys. Union monogr.* 16, 191–209.
Heard, H. C. & Raleigh, C. B. 1972 Steady-state flow in marble at 500° to 800°C. *Geol. Soc. Am. Bull.* **83**, 935–956.
Henniker, J. C. 1949 Depth of the surface zone of a liquid. *Rev. Mod. Phys.* **21**, 322–342.
Hobbs, B. E. 1968 Recrystallisation of single crystals of quartz. *Tectonophysics* **6**, 353–401.
Holland, H. D. 1967 Gangue minerals in hydrothermal deposits. In *Geochemistry of hydrothermal ore deposits* (ed. H. L. Barnes). New York: Holt, Rinehart & Winston.
Jost, W. 1960 *Diffusion in solids, liquids and gases*. New York: Academic Press.
Kats, A. 1962 Hydrogen in α-quartz. *Philips Res. Rep.* **17**, 133–279.
Kennedy, G. C. 1950 A portion of the system silica-water. *Econ. Geol.* **45**, 629–653.
Kerrich, R. 1975 Ph.D. Thesis, University of London.
Lawson, A. W. & Hughes, A. J. 1963 High pressure properties of water. In *High pressure physics and chemistry* (ed. R. S. Bradley), pp. 207–225. London: Academic Press.
McGregor, R. 1974 *Diffusion and sorption in fibres and films*. New York: Academic Press.
Nye, J. F. 1953 The flow law of ice from experiments in glacier tunnels, laboratory experiments and the Jungfraufirn borehole experiment. *Proc. R. Soc. Lond.* A **219**, 477–489.
Olejnick, S., Stirling, G. C. & White, J. W. 1970 Neutron scattering studies of layer silicates. In Thin liquid films and boundary layers. *Spec. Discuss. Faraday Soc.* **1**, 194–201.
Paterson, M. S. 1973 Non-hydrostatic thermodynamics and its geologic applications. *Rev. Geophys. Space Phys.* **11**, 355–389.
Price, N. J. 1970 Laws of rock behaviour in the earth's crust. In *Symposium on rock mechanics, 11th, Berkeley, California*; Am. Inst. Mining Metall. and Petroleum Engineers (ed. H. Somerton), pp. 3–23.
Price, N. J. 1975 Rates of deformation. *Q. J. geol. Soc. Lond.* (In the Press.)
Raj, R. & Ashby, M. F. 1971 On grain boundary sliding and diffusional creep. *Metall. Trans.* **2**, 1113–1126.
Raleigh, C. B. & Kirby, S. H. 1970 Creep in the upper mantle. *Mineral Soc. Am. Spec. Pap.* **3**, 183–190.
Ramsay, J. G. 1967 *Folding and fracturing of rocks*. New York: McGraw-Hill.
Roberts, A. D. & Tabor, D. 1970 Mechanical properties of very thin surface films. In Thin liquid films and boundary layers. *Spec. Discuss. Faraday Soc.* **1**, 243–250.
Rutter, E. H. 1974 The influence of temperature, strain-rate and interstitial water in the experimental deformation of calcite rocks. *Tectonophysics* **22**, 311–334.
Sharp, W. E. & Kennedy, G. C. 1965 The system CaO–CO_2–H_2O in the two phase region calcite and aqueous solution. *J. Geol.* **73**, 391–403.
Smith, F. G. 1963 *Physical geochemistry*. Reading, Massachussetts: Addison-Wesley.
Sorby, H. C. 1855 On slaty cleavage, as exhibited by the Devonian limestones of Devonshire. *Phil. Mag.* **11**, 20–37.
Stephen, H. 1963 Solubility of inorganic and organic compounds. London: Pergamon.
Stocker, R. L. & Ashby, M. F. 1973 On the rheology of the upper mantle. *Rev. Geophys. and Space Phys.* **11**, 391–421.
Tullis, J., Christie, J. M. & Griggs, D. T. 1973 Microstructures and preferred orientations of experimentally deformed quartzites. *Geol. Soc. Am. Bull.* **84**, 297–314.
Ward, S. H. & Fraser, D. C. 1967 Conduction of electricity in rocks. In *Mining geophysics, Vol. 2, Theory* (ed. D. A. Hansen). Tulsa, Oklahoma: Society of Exploration Geophysicists.
Weertman, J. 1968 Dislocation climb theory of steady-state creep. *Am. Soc. Metals Trans.* **61**, 681–694.
Weertman, J. 1970 The creep strength of the earth's mantle. *Rev. Geophys.* **8**, 145–168.
Weyl, P. K. 1959 Pressure solution and force of crystallisation – a phenomenological theory. *J. geophys. Res.* **64**, 2001–2025.
White, S. 1971 Hydroxyl ion diffusion in quartz. *Nature, Phys. Sci.* **230**, 192.
White, S. 1975 Strain and the development of deformation features in quartz tectonites. *Phil. Trans. R. Soc. Lond.* A **283**, 69–86 (this volume).
Zen, E-an 1957 Partial molar volumes of some salts in aqueous solutions. *Geochim. Cosmochim. Acta* **12**, 103–122.

PHILOSOPHICAL TRANSACTIONS OF THE ROYAL SOCIETY A MATHEMATICAL, PHYSICAL & ENGINEERING SCIENCES

Discussion

D. Elliott (*The Johns Hopkins University, Dept. Earth & Planetary Sci., Balto., Md, U.S.A.*). (1) Diffusive mass transfer occurs through the volume of crystal lattice, along grain boundaries, and through the fluid phase in pores. These three diffusion paths could all produce fabrics which for the past century geologists have called 'pressure solution'. Is Dr Rutter attempting to restrict this useful and well understood term entirely to diffusion via pores?

(2) Does the author define pores and grain boundaries in a way which takes into account the clear differences in bonding, microstructure, and thermodynamic properties which exist between these diffusion paths?

(3) The existence of pores can be proven by drusy cavity-filling textures with euhedral crystal terminations; but none of the photomicrographs shown in the lecture demonstrated such pores. Has the author some other evidence for choosing pore space diffusion rather than grain boundary diffusion?

(4) Deformation mechanism maps are an interesting example of the parallel development of a similar notion in two different sciences, since my and Ashby's concepts of these plots were both submitted to different journals in 1972 and were developed quite independently of each other. The main difference is that I used grain size as one of the coordinates while Ashby used stress. Three dimensional maps are unlikely ever to find wide acceptance. There are distinct advantages to using grain size as a coordinate, since such deformation mechanism maps are composed of straight rather than curved boundaries and are far easier to construct. Further, deviatoric stresses during tectonic deformation are unlikely to vary by much more than 1 lg unit (2.5–25 MPa), and the author's deformation mechanism maps vary over a very large number of log units. Has the author some reasons for rejecting deformation mechanism maps using grain size as a coordinate?

E. H. Rutter. Dr Elliott's first three questions can be dealt with together. He has himself pointed out (Elliott 1973) that Coble creep, Nabbarro–Herring creep and what geologists call pressure solution are, from a geometric standpoint, essentially the same. They will each produce the same texture. However, such textures develop in rocks deformed at temperatures which are very low (*ca.* 200–400 °C) compared with the higher temperatures we might expect to be necessary for even Coble creep to take place in rocks at a geologically significant strain rate at a given grain size. It is therefore reasonable to suppose that the rate at which the intergranular diffusion process occurs at such temperatures is enhanced by the presence of a solution phase in the grain boundaries. In my model I am *not* concerned with pore diffusion. I assume that the deformation rate controlling process is diffusion in grain boundaries which can support shear stress, and I have attempted to take into account the special properties of thin liquid films in stressed interfaces in estimating diffusion behaviour. The other components of the deformation process – solution kinetics, pore diffusion rates and precipitation kinetics are all assumed to be relatively rapid. The isotopic tracer experiments have at least shown that pore diffusion is too rapid to be deformation rate controlling. I think Dr Elliott may have misunderstood me, judging from these questions, which imply that I was *particularly* concerned with pore diffusion.

Turning now to the question of the most suitable method of representing deformation mechanism fields on a graph, it follows from the form of the constitutive flow laws for thermally activated flow processes that from grain size, temperature, stress and strain rate we can choose

any pair for axes and contour with respect to a third. A separate set of graphs is needed to take into account variations in the fourth. The choice must be determined by the use to which the map is to be put. Dr Elliott proposed a plot of log grain size against reciprocal absolute temperature. Mohamed & Langdon (1974) have proposed a plot of log grain size (grain size normalized by dividing by a Burgers vector) against log stress, and Weertman (1968) and Ashby (1972) proposed the log stress against homologous temperature (T/T_m) plot. Both Elliott's and Mohamed & Langdon's plots led to straight line boundaries between deformation mechanism fields, whereas Ashby's leads to some boundaries being curved, but I do not think that this is important and I do not believe that any one diagram is more difficult to construct than any other type.

A great deal of space has been devoted in the literature to emphasizing the importance of stress and temperature in *all* the thermally activated deformation processes, whereas grain size is generally believed to be of particular importance only in diffusive mass transfer flow processes. The concepts of theoretical shear strength at *ca.* $\sigma = 10^{-1}\,G$, the transition from dislocation glide to dislocation creep at *ca.* $\sigma = 10^{-3}\,G$ and a lower limit of $10^{-5}\,G$ as the minimum stress for dislocation motion, over a wide temperature range, mean that stress is a logical choice of variable for one axis. The use of homologous temperature for the other axis serves to emphasize, for example, that the transition from work hardening flow to steady state flow at laboratory strain rates occurs at *ca.* $T = 0.5\,T_m$ for virtually all materials. The principal effect of a grain size change is to shift the lower bound of the dislocation creep field upwards as grain size is reduced (see also White, this volume) and to increase the importance of Coble creep, the position of the dislocation glide/dislocation creep fields boundary remaining unchanged. Because the dislocation glide and diffusive mass transfer flow fields do not intersect except at low temperatures and low strain rates, the relative positions of these fields cannot be represented satisfactorily on a map where grain size is one of the axes. For these reasons I believe that the Ashby plot can convey more information more succinctly than any other type of diagram, and it is therefore more easily appreciated by geologists in the present state of development of the subject.

References

Ashby, M. F. 1972 A first report on deformation mechanism maps. *Acta Metall.* **20**, 887–897.
Elliott, D. 1973 Diffusion flow laws in metamorphic rocks. *Geol. Soc. Am. Bull.* **84**, 2645–2664.
Mohamed, F. A. & Langdon, T. G. 1974 Deformation mechanism maps based on grain size. *Metall. Trans.* **5**, 2339–2345.
Weertman, J. 1968 Dislocation climb theory of steady state creep. *Am. Soc. Metals Trans.* **61**, 681–694.

PHILOSOPHICAL TRANSACTIONS OF THE ROYAL SOCIETY A MATHEMATICAL, PHYSICAL & ENGINEERING SCIENCES